Synthesis, Characterization, and Control Release of Zinc Layered Nitrate Intercalated with Beta-Napthoxyacetic Acid (BNOA) Nanocomposite

Hasnatul Fitriah Abd Rahim, Mohd Noor Jalil, Faeiza Buyong, Siti Halimah Sarijo, and Hamizah Mohd Zaki*

School of Chemistry and Environment, Faculty of Applied Sciences, Universiti Teknologi MARA, Shah Alam, Selangor 40450, Malaysia

** **Corresponding author:***

email: hamiz410@uitm.edu.my

Received: August 29, 2023
Accepted: October 22, 2023

DOI: 10.22146/ijc.88459

Abstract: *In this research, the synthesis of the host using zinc nitrate-hexahydrate as a precursor to form zinc layered nitrate (ZLN) and the guest anion which is beta-napthoxyacetic acid (BNOA) will be intercalated with the ZLN to produce nanocomposites called ZLN/beta-napthoxyacetic acid (ZLNB). The method used for the synthesis of the host was self-assembly and ion exchange. The nanocomposites were confirmed with the basal spacing increases from 9.8 to 28.2 Å by using powder X-ray diffraction (PXRD). Therefore, proved the bigger basal spacing compared to the layered double hydroxide of MgAl and ZnAl. The appearance of the FTIR shift band at 1603 cm^{-1} of C=C aromatic ring indicates that the anions have been successfully incorporated into the interlayers of ZLNB. Moreover, the loading percentage estimated by the carbon content from the ZLNB determined by CHNS analyzer was 41.8% (w/w). The morphology analysis confirmed the plate-like structure for ZLN into flaky-like with irregular, porous and unambiguous structure for ZLNB by field emission scanning electron microscopy (FESEM). The controlled release property showed that the release of BNOA in the various aqueous solutions is in the order of Na_3PO_4 > Na_2SO_4 > NaCl and fitted into pseudo-second-order kinetic models.*

Keywords: *beta-napthoxyacetic acid (BNOA); control release; zinc layered nitrate*

■ INTRODUCTION

Research on nanotechnology has discovered the uniqueness of zinc layered hydroxide (ZLH), which is a type of layered double hydroxide (LDH) that has been widely studied in recent years due to its distinctive properties and potential applications in various fields [1]. LDHs are two-dimensional, positively charged layered materials that can intercalate anions between the layers. ZLH specifically is composed of sheets of zinc cations and hydroxide anions, with interlayer spaces that can accommodate various anions, such as carbonate, nitrate, sulfate, and organic anions [2]. The notable advantages of ZLH are its large surface area, facilitating effective adsorption of anions and organic compounds. Furthermore, the interlayer spacing and surface charge of the material can be altered using diverse synthesis methods, rendering it a versatile substance with wide-ranging applications [3].

Extensive research on ZLH has been established on its distinctive characteristics and wide range of potential uses, particularly in enhancing the efficiency and stability of agrochemicals and minimizing the adverse environmental effects associated with traditional agrochemical formulations [4]. In this research, the zinc layered nitrate (ZLN) will be intercalated with beta-naphtoxyacetic acid (BNOA) (Fig. 1), which is an auxin under the subgroup of plant growth regulators. The auxins are pivotal in promoting root development and the effectiveness of cutting propagation. The application of auxin-based formulations (such as rooting hormones) will encourage root growth in plant cuttings thus facilitating the establishment of new plants [5]. The potential of the synthesized nanocomposites holds promise in the field of agrochemical technology as it can serve as a carrier for controlled-release formulations by utilizing the interlayer spaces of ZLN, such that the BNOA

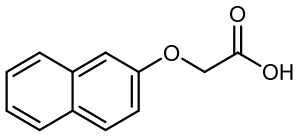

Fig 1. Chemical structure of BNOA

can be accommodated and gradually released over time. This controlled-release mechanism significantly improves the effectiveness of agrochemicals, thereby reducing the required amount for weed control and minimizing the risk of environmental contamination [1,6].

Apart from that, ZLH has also been the subject of an investigation regarding its capacity to absorb heavy metals and other pollutants from agricultural environments such as soil and water [7]. Moreover, ZLH demonstrates the potential to enhance the stability and solubility of agrochemicals, leading to prolonged shelf-life and increased effectiveness. By incorporating ZLH, formulations can be developed with heightened resistance to degradation, reducing the frequency of agrochemical applications and consequently lessening the environmental impact [8].

In summary, ZLH exhibits considerable potential for advancing agrochemical technology by improving the efficacy, stability, and environmental implications of conventional formulations. Continued research in this field is expected to unveil new and innovative applications of ZLH in agrochemical technology.

■ EXPERIMENTAL SECTION

Materials

Ethanol (C_2H_5OH, 95.0%) was purchased from R&M Chemical (Da, United Kingdom). Zinc chloride ($ZnCl_2$, 95.0%), was purchased from Systerm, while zinc nitrate hexahydrate($Zn(NO_3)_2{\cdot}6H_2O$, 98.0%) was obtained from Bendosen. Sodium hydroxide (NaOH, 99.0%), sodium chloride (NaCl, 99.5%), sodium sulphate (Na_2SO_4, 99.5%), and sodium phosphate (Na_3PO_4, 99.5%) were obtained from R&M Chemicals (Da, United Kingdom) and 2-naphthoxyacetic acid ($C_{12}H_{10}O_3$, 98.0%) was purchased from Sigma-Aldrich (Hamburg, Germany). All the chemicals were used without further purification. All solutions were prepared using deionized water.

Instrumentation

The powder X-ray diffraction (PXRD) patterns of the samples were recorded on a PANalytical X'pert PRO XRD (USA) using Cu Kα radiation (λ = 1.5406 Å) at 40 kV and 30 mA. The data were collected in the range of 2θ = 2–60° with a scanning rate of 2°/s. The Fourier transform infrared (FTIR) absorption spectrum of each sample was obtained by a KBr pellet method and recorded over the range of 450–4000 cm^{-1} on a Perkin Elmer Spectrum 1725X (USA). The surface morphology of the materials was characterized by using field emission scanning electron microscopy (FESEM) (Carl Zeiss Supra 40, USA) at 10,000 magnifications. A CHNS analyzer 2400 PerkinElmer Series II (USA) with a dynamic flash combustion technique was used to determine the loading percentage of the nanocomposite.

Procedure

The synthesis involved using various chemicals obtained from different suppliers without additional purification. Initially, a 50 mL solution containing 0.069 mol of $Zn(NO_3)_2{\cdot}6H_2O$ was prepared by slowly adding 0.75 M NaOH while maintaining a pH of 7.0 ± 0.2 under magnetic stirring in the presence of N_2 gas. The resulting product was then subjected to centrifugation, washed with deionized water, and dried in an oven at 70 °C for 48 h [9].

Next, 0.8 g of ZLN was mixed with a 20 mL (0.15 M) solution of 2-napthoxyacetic Acid (BNOA) and adjusted to a pH of 7.5 ± 0.2 by slowly adding 0.75 M NaOH under magnetic stirring in the presence of N_2 gas. The solution was aged for 18 h in an oil bath shaker at 70 °C [10-11]. The resulting product, ZLN/2-napthoxyacetic acid (ZLNB), was then centrifuged, thoroughly washed with deionized water, and dried in an oven for 24 h.

■ RESULTS AND DISCUSSION

Powder XRD Analysis

Fig. 2 shows the PXRD patterns of ZLN and the nanocomposite, ZLNB were synthesized by using the ion exchange method.

The PXRD pattern of the basal spacing for ZLN (Fig. 2) with nitrate as interlamellar anions is 9.8 Å, which

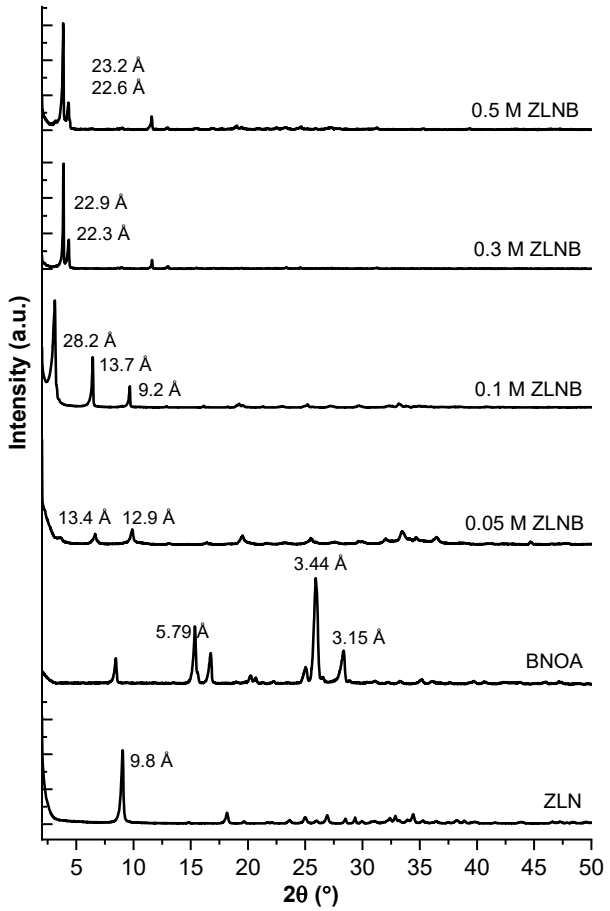

Fig 2. PXRD pattern for ZLN, BNOA and ZLNB ranging from 0.05 to 0.50 M

is in agreement with previous researchers [9]. The resultant nanocomposite of 0.1 M ZLNB (Fig. 2), with the enlarged basal spacing of 28.2 Å had a well-ordered nanolayered structure compared to the other concentrations. The enlarged basal spacing was bigger than MgAl (20.3 Å) or ZnAl (19.5 Å) published elsewhere [10]. The increase in basal spacing ensured that the guest anions, BNOA was successfully intercalated into the interlayer of ZLN as well as increased the capacity of BNOA loading. These patterns also exhibit some features of layered materials such as narrow, symmetric, with high-intensity peaks at low 2θ values indicating a good crystallinity of nanocomposite phase was obtained [11]. Thus, nanocomposite prepared using 0.1 M ZLNB was subsequently used for further characterization.

FTIR Study

The FTIR spectra for ZLN, BNOA and ZLNB ranging from 0.05 to 0.50 M are shown in Fig. 3. A characteristic peak of ZLN at around 3497 cm^{-1} which was attributed to OH stretching due to the presence of a hydroxyl group. The appearance of a strong absorption band at 1384 cm^{-1} was attributed to the presence of NO_3 in the interlayer of ZLN [12]. Then, the BNOA spectra showed a strong band at 1746 cm^{-1} of the carbonyl (C=O) stretching vibration. The band at 1629 cm^{-1} due to the vibration stretching of C=C aromatic rings. The other intense band at 1223 cm^{-1} shows the stretching of C–O–C while the band at 749–909 cm^{-1} is due to phenyl ring substitution [13].

The FTIR patterns of ZLNB display a combination of the ZLN and BNOA spectra, showcasing the coexistence of both functional groups within ZLNB. The absence of the 1384 cm^{-1} absorption band that was attributed to nitrate ions showed that the BNOA anion had fully replaced the nitrate ions. This shows that BNOA has a stronger attraction to the inorganic interlamellar region compared to nitrate anions, establishing its occupancy within the interlamellar layer between the inorganic layers.

The most significant feature in the FTIR spectra is the disappearance of band 1746 cm^{-1} of carboxylic acid. The absorption band formed at around 1616 cm^{-1}, which is attributed to carboxylate ions (COO^-), confirmed the presence of BNOA in the anionic form in the interlayer of the LDH [14]. These FTIR results supplement the PXRD findings, which validate the formation of BNOA

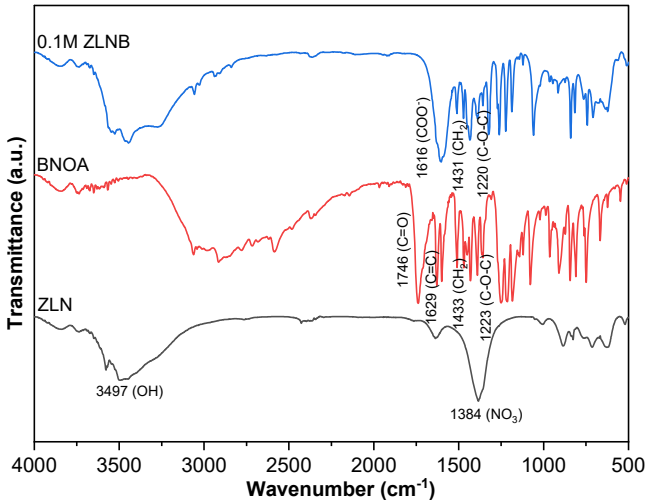

Fig 3. FTIR spectra of ZLN, BNOA, and 0.1 M ZLNB

within the ZLN layer, resulting in the creation of ZLNB nanocomposites.

Morphological Study

The morphological surface of ZLN and ZLNB was displayed in Fig. 4 at a magnification of 10,000×. The ZLC (Fig. 4(a)) had a plate-like structure morphology, which correlated with the morphology of ZLH and was in agreement with previous study [15]. The nanocomposites ZLNB (Fig. 4(b)), show a flaky-like with irregular, porous and unambiguous structure compared to ZLN [16]. The agglomerations of ZLNB indicate that the anions had successfully incorporated into the ZLN, which correlates with the expanding basal spacing of the nanocomposites, ZLNB increases as proved in PXRD analysis (Fig. 2).

Elemental Analysis

The intercalation of BNOA anions into the ZLN inorganic interlayer was also confirmed by the elemental analysis (CHNS). Table 1 shows the percentage of C (carbon), H (hydrogen), and N (nitrogen) in ZLN and ZLNB. The percentage of C increased from 0.2% (ZLN) to 28.2% (ZLNB) indicating that the presence of the anions, while the percentage of N decreased from 5.1% (ZLN) to 0.3% (ZLNB) ensured that the nitrates ions were replaced by guest anions, BNOA during the intercalation process. Then, the percentage loading of BNOA anions was 41.8% (w/w) for ZLNB, which was estimated from the carbon content in the nanocomposite [13].

Surface Properties – Isotherm, Surface Area and Pore Distribution

Fig. 5 shows the graph of isotherm and pore distribution of ZLN and ZLNB, while Table 2 presents a summary of the chemical composition, surface area, and pore volume for ZLN and ZLNB. The table provides information regarding the surface properties which successfully underwent intercalation of BNOA at an optimal concentration of 0.1 M ZLNB. These values were determined using the Brunauer, Emmet, and Teller (BET) method, as well as the Barret, Joyner, and Halenda (BJH) method.

Based on the IUPAC classification, both ZLN and ZLNB isotherms can be categorized as Type IV, specifically belonging to the mesopore classification. The desorption hysteresis exhibits a type H3 loop, indicating the presence of flake-like particles that form slit-shaped pores, which align with the surface morphology depicted in Fig. 4 [17]. Noted that the absence of any adsorption limitation at high P/P_0 suggests the absence of macropores in the nanocomposites following the intercalation process.

According to the adsorption isotherm shown in Fig. 5, the initial phase involves monolayer adsorption on the surface of the pores at low partial pressures. As the partial pressures increase, the formation of multilayers

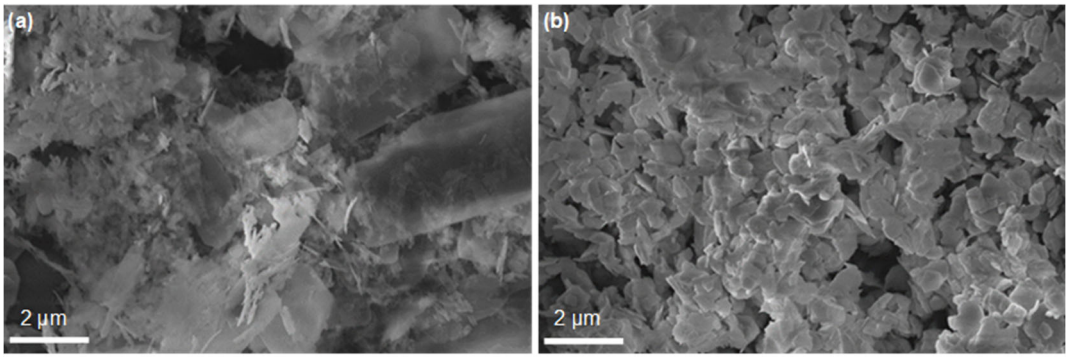

Fig 4. Surface morphology of (a) ZLN and (b) ZLNB with 10,000× magnification

Table 1. Elemental analysis of ZLN and ZLNB

Sample	Basal spacing (Å)	% C	% H	% N	% Loading
ZLN	9.8	0.2	1.6	5.1	-
ZLNB	28.2	29.8	2.9	0.3	41.8

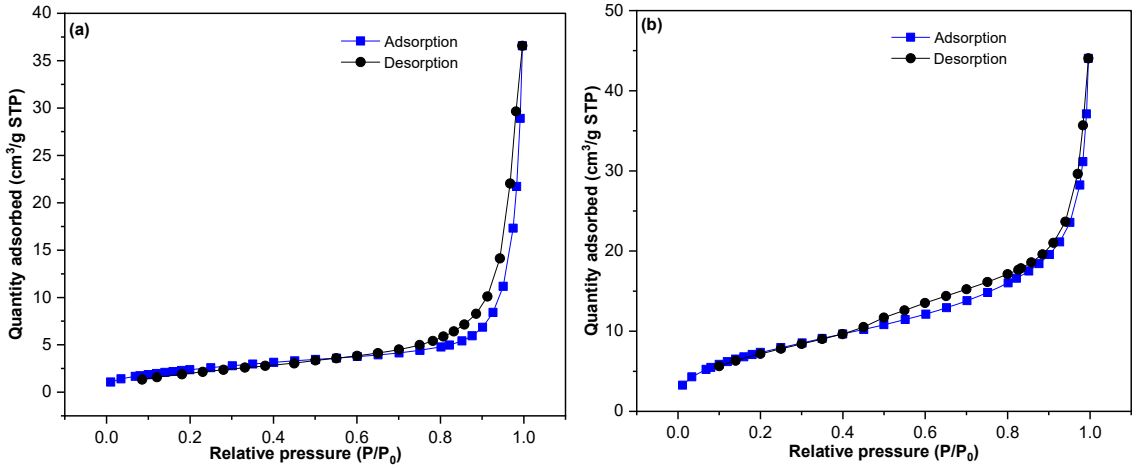

Fig 5. Nitrogen adsorption-desorption isotherm of (a) ZLN and (b) ZLNB

takes place. Nitrogen shows a gradual uptake in the pore volumes within the range of 0.00 to 0.04 cm^3/g, reaching a maximum adsorbate uptake of 0.04 cm^3/g for ZLN (Fig. 5(a)) and 0.03 cm^3/g for ZLNB (Fig. 5(b)). No limitations were observed in the desorption of nitrogen gas at high partial pressures. However, the desorption isotherm displayed a hysteresis loop, indicating capillary condensation occurring within the mesopores, persisting until a partial pressure of approximately 0.75 (P/P_0) for ZLNB [18]. This demonstrates a correlation between the increase in surface area and alteration of pore size from ZLN to ZLNB, confirming the successful intercalation process involving the insertion of BNOA.

Based on Fig. 6 and the summary in Table 2 shown, the initial surface area of ZLN was 9.16 m^2/g, but it increased to 28.05 m^2/g. Similarly, the BJH pore volume for ZLN was 0.04 cm^3/g, which slightly increased to 0.05 cm^3/g in ZLNB. This observation provides further evidence of the successful intercalation of BNOA within the interlayer of the lamella. Additionally, the surface morphology in Fig. 2 reveals that the intercalation process has brought about changes in the pore texture of the ZLN and ZLNB, as indicated by the variation in peak value and pore diameter observed in the pore size distribution between the host and the intercalated nanocomposites.

This demonstrates that the surface morphology, elemental analysis outcomes, and the investigated surface properties affiliate with the PXRD pattern and FTIR studied, providing confirmation of the intercalation of BNOA into the ZLN layer to form ZLNB.

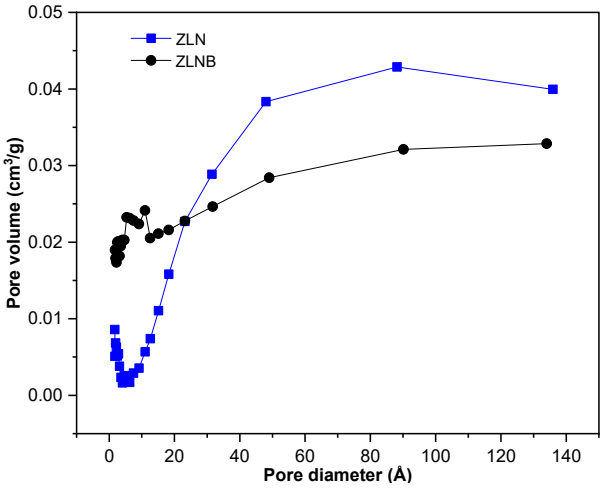

Fig 6. Pore distribution of ZLN and ZLNB

Table 2. Elemental analysis, surface area, pore distribution of ZLN and ZLNB

Sample	C (%w/w)	H (%w/w)	Percentage loading (%)	BET Surface area (m^2/g)	BJH Desorption pore diameter (Å)	BET average pore volume (cm^3/g)
ZLN	0.28	1.61	-	9.16	202.20	0.04
ZLNB	29.82	2.99	41.80	28.05	83.50	0.05

Control Release Study

Fig. 7 shows the control release percentage of BNOA in the ZLNB into the various solutions of 0.005 M of Na_3PO_4, Na_2SO_4, and NaCl The release of BNOA from ZLNB exhibited a rapid rate during the initial 3 h, followed by a slower rate until reaching equilibrium around 12 h, as illustrated in Fig. 7. It was observed that the highest amount of BNOA was released from ZLNB in the solution containing Na_3PO_4. However, in NaCl solution, the lowest amount of BNOA was released. Specifically, at the end of the rapid release phase, the Na_3PO_4, Na_2SO_4, and NaCl solutions accounted for 36%, 26%, and 14%, respectively. Thus, the order of BNOA release from ZLNB after 36 h was summarized as Na_3PO_4 > Na_2SO_4 > NaCl. This result is in agreement with the previous study [19].

These results indicate that the affinity of phosphate (PO_4^{3-}), sulfate (SO_4^{2-}), and chloride (Cl^-) ions towards the inorganic interlayer of all nanocomposites follows a specific order. This suggests that the affinity of the incoming anion plays a significant role in determining the percentage of the saturated release of the anion from the nanocomposite into the aqueous solution. In other words, the ion exchange process is governed by the affinity of the anion to be exchanged, which determines the amount of the guest anion, BNOA, that will be released [14].

Kinetic Study

The control release data obtained from the quantitative analysis, as depicted in Fig. S1-S3, were subjected to fitting using zeroth-order, first-order, and pseudo-second-order functions. It was proposed that the dissolution of ZLNB could serve to control the release of anions. Previous studies on the release kinetics of intercalated ZLH employed a single straight line to fit the experimental data.

Below are the equations for the zeroth-order (Eq. (1)), first-order (Eq. (2)), and pseudo-second-order (Eq. (3)) functions, where C_{eq} represents the percentage release of herbicides at equilibrium, C_t represents the percentage release at time t, and c is a constant [20].

$$C_t = kt + c \quad (1)$$

$$-\log(1 - C_t) = kt + c \quad (2)$$

$$t/C_t = 1/kC^2_{eq} + (1/C_{qe})t \quad (3)$$

Based on the data presented in Table 3, the release of BNOA into 0.005 M Na_3PO_4, Na_2SO_4 and NaCl, and aqueous solutions were analyzed using zeroth-order, first-order, and pseudo-second-order kinetic models within the release time range of 0–2160 min. The zero-order kinetic model demonstrated poor fitting of the data, with regression values approximately around 0.6000 to 0.9000 in the solutions. In contrast, the first-order kinetic model exhibited better fitting, with regression values around 0.8000 to 0.9000 for each solution. Then, the release profiles displayed the best fitting to the pseudo-second-order kinetics during the longer time range process of 2160 min, with regression values close to 1.000 for all solutions.

The release of BNOA from the inorganic ZLN interlamellar involved both the dissolution of the nanocomposite and the ion exchange between the intercalated anions within the interlamellar space with chloride, sulfate, and phosphate anions present in the aqueous solution [21]. This entire release process followed a pseudo-second-order kinetic model, as indicated by the regression values (r^2). Specifically, the release of BNOA from the ZLNB nanocomposite was well-fitted with the pseudo-second-order model. The release of guest anion in this process is influenced by the concentration of the solution and time, with lower

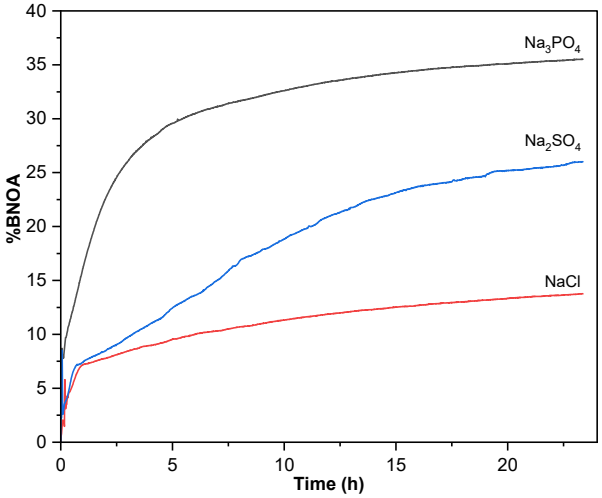

Fig 7. Release the percentage of BNOA in the ZLNB into various solutions (Na_3PO_4, Na_2SO_4 and NaCl)

Table 3. The percentage of control release and kinetic release rate of BNOA in ZLNB

Sample	Media	Saturated release (%)	Correlated coefficient (r^2)			Rate constant of 2nd order, k (L/mg min)
			Zeroth-order	First-order	Pseudo-second-order	
ZLNB	Na_3PO_4	36	0.6366	0.9813	0.9996	7.2567×10^{-3}
	Na_2SO_4	26	0.8532	0.8541	0.9931	3.5852×10^{-3}
	NaCl	14	0.9367	0.8804	0.9616	1.1775×10^{-3}

solution concentrations resulting in shorter release times until reaching equilibrium [22].

In addition, the exchange of chloride, sulfate, and phosphate ions from the solution demonstrates the strong ion exchange capacity of ZLNB. According to the release profile of BNOA depicted in Fig. 6, the presence of anions in the soil water displaces other cations and exchanges places within the interlayer of ZLNB. Consequently, ZLNB is capable of absorbing nutrients provided by the soil through cation exchange capacity (CEC) and facilitating the uptake by plant roots via the simplistic pathway towards the root xylem [23]. The kinetic release rate for all anions into the release media was also in the order of $Na_3PO_4 > Na_2SO_4 > NaCl$, as shown in the k values as summarized in Table 3.

■ CONCLUSION

The findings revealed a strong correspondence among the different characterizations conducted. Firstly, the FTIR analysis confirmed the successful insertion of BNOA into the basal spacing of ZLN. The presence of BNOA functional groups, such as carboxylate ions, and the absence of nitrate ions in ZLN were evident in the resulting ZLNB nanocomposite. Furthermore, the PXRD analysis supported the expansion of the basal spacing in ZLNB, as it increased from 9.8 to 28.2 Å due to the inclusion of BNOA. The estimated loading percentage of BNOA in ZLNB was approximately 41.8% (w/w). Elemental analysis also substantiated the effective integration of BNOA into the interlayer of ZLNB. Moreover, nitrogen adsorption-desorption isotherms of both ZLN and ZLNB displayed a type IV pattern with a type H3 hysteresis loop, characteristic of mesoporous materials. This pattern supported the consistent interlayer spacing in ZLNB. Surface property investigations revealed an augmentation in surface area from ZLN to ZLNB, which was also affirmed by FESEM analysis, indicating a transition from flake-like particles to aggregated slit-shaped pores in ZLNB. The analysis of slow-release kinetics demonstrated that the pattern of anion release from the aqueous solution, influenced by ion exchange phenomena, governed the release of BNOA into NaCl, Na_2SO_4, and Na_3PO_4 solutions. The kinetics of slow release followed a pseudo-second-order model, with a regression value close to 1.000. This suggested that the increased basal spacing facilitated the exchange of BNOA with anions (PO_4^{3-}, SO_4^{2-}, and Cl^-) based on their electric charge selectivity.

■ ACKNOWLEDGMENTS

The authors would gratefully acknowledge Universiti Teknologi Mara (UiTM Shah Alam) for the financial support through LESTARI grant 600-RMC/MYRA/5/3/LESTARI (107/2020) and FRGS/1/2021/STG05/UITM/02/30.

■ CONFLICT OF INTEREST

All the authors do not have conflict of interest.

■ AUTHOR CONTRIBUTIONS

Hasnatul Fitriah Abd Rahim carried out the experiment, analyzed the findings, and wrote the manuscript. Hamizah Mohd Zaki outlined the methodology, results, and interpretations. Mohammad Noor Jalil provided contextual information and revised the manuscript. Siti Halimah Sarijo contributed original ideas and insights to the field of study. Faeiza Buyong adhered to academic norms and formatting guidelines in writing. All authors agreed to the final version of this manuscript.

■ REFERENCES

[1] Benício, L.P.F., Silva, R.A., Lopes, R.A., Eulálio, D., dos Santos, R.M.M., de Aquino, L.A., Vergütz, L., Novais, R.F., da Costa, L.M., Pinto, F.G., and

Tronto, J., 2015, Layered double hydroxides: Nanomaterials for applications in agriculture, *Rev. Bras. Cienc. Solo*, 39 (1), 1–13.

[2] Mallakpour, S., Hatami, M., and Hussain, C.M., 2020, Recent innovations in functionalized layered double hydroxides: Fabrication, characterization, and industrial applications, *Adv. Colloid Interface Sci.*, 283, 102216.

[3] Forano, C., Costantino, U., Prévot, V., and Gueho, C.T., 2013, Layered double hydroxides (LDH), *Dev. Clay Sci.*, 5, 745–782.

[4] Ahmad, R., Hussein, M.Z., Wan Abdul Kadir, W.R., Sarijo, S.H., and Yun Hin, T.Y., 2015, Evaluation of controlled-release property and phytotoxicity effect of insect pheromone zinc-layered hydroxide nanohybrid intercalated with hexenoic acid, *J. Agric. Food Chem.*, 63 (51), 10893–10902.

[5] Bratovcic, A., Hikal, W.M., Said-Al Ahl, H.A.H., Tkachenko, K.G., Baeshen, R.S., Sabra, A.S., and Sany, H., 2021, Nanopesticides and nanofertilizers and agricultural development: Scopes, advances and applications, *Open J. Ecol.*, 11 (4), 301–316.

[6] Muharam, S., Fitri, A., Yuningsih, L.M., Putri, Y.M.T.A., and Rahmawati, I., 2020, Synthesis and characterization of controlled-release urea fertilizer from superabsorbent hydrogels, *Indones. J. Chem.*, 20 (3), 616–625.

[7] Dong, Y., Kong, X., Lou, X., and Wang H., 2022, Adsorptive removal of heavy metal anions from water by layered double hydroxide: A review, *Chemosphere*, 303, 134685.

[8] Zobir, S.A., Ali, A., Adzmi, F., Sulaiman, M.R., and Ahmad, K., 2021, A review on nanopesticides for plant protection synthesized using the supramolecular chemistry of layered hydroxide hosts, *Biology*, 10 (11), 1077.

[9] Hashim, N., Muda, Z., Md Isa, I., Mohd Ali, N., Abu Bakar, S., and Hussein, M.Z., 2017, The effect of ion exchange and co-precipitation methods on the intercalation of 3-(4-methoxyphenyl)propionic acid into layered zinc hydroxide nitrate, *J. Porous Mater.*, 25 (1), 249–258.

[10] Abd Rahim, H.F., Mohd Zaki, H., Jalil, M.N., and Sarijo, S.H., 2023, Synthesis of zinc layered hydroxide with 2-napthoxyacetic acid (BNOA) with chloride as counter ions via ion exchange method, *J. Mater. Phys. Chem.*, 11 (2), 29–37.

[11] Mohd Sharif, S.N., Hashim, N., Md Isa, I., Mohd Ali, N., Abu Bakar, S., Hussein, M.Z., Mamat, M., Abu Bakar, N., and Wan Mahamod, W.R., 2018, Preparation and characterisation of novel paddy cultivation herbicide nanocomposite from zinc/aluminium layered double hydroxide and quinclorac anion, *Mater. Res. Innovations*, 23 (5), 260–265.

[12] Khadiran, N.F., Hussein, M.Z., Ahmad, R., Khadiran, T., Zainal, Z., Wan Abdul Kadir, W.R., and Hashim, S.S., 2021, Preparation and properties of zinc layered hydroxide with nitrate and phosphate as the counter anion, a novel control release fertilizer formulation, *J. Porous Mater.*, 28 (6), 1797–1811.

[13] Li, S., Shen, Y., Xiao, M., Liu, D., and Fan, L., 2019, Synthesis and controlled release properties of β-naphthoxyacetic acid intercalated Mg–Al layered double hydroxides nanohybrids, *Arabian J. Chem.*, 12 (8), 2563–2571.

[14] Jubri, Z., Mohd Yusoff, N.Z.A., Sarijo, S.H., Marsom, E.S., and Hussein, M.Z., 2017, Synthesis, characterization and controlled release properties of zinc–aluminium-beta-naphthoxyacetate nanocomposite, *J. Porous Mater.*, 24 (3), 573–582.

[15] Zhu, J., Zhu, Z., Zhang, H., Lu, H., Zhang, W., Qiu, Y., Zhu, L., and Küppers, S., 2018, Calcined layered double hydroxides/reduced graphene oxide composites with improved photocatalytic degradation of paracetamol and efficient oxidation-adsorption of As(III), *Appl. Catal., B*, 225, 550–562.

[16] Adam, N., Sheikh Mohd Ghazali, S.A.I., Dzulkifli, N.N., and Che Hak, C.R., 2021, Characterization, physiochemical, controlled release studies of zinc–aluminium layered double hydroxide and zinc layered hydroxide intercalated with salicylic acid, *Bull. Mater. Sci.*, 44 (2), 155.

[17] Stepanova, L.N., Belskaya, O.B., Vasilevich, A.V., Gulyaeva, T.I., Leont'eva, N.N., Serkova, A.N., Salanov, A.N., and Likholobov, V.A., 2020, The study of structural, textural and basic properties of MgAl- and LiAl-LDH prepared by mechanochemical method, *Catal. Today*, 357, 638–645.

[18] Mohd Sharif, S.N., Hashim, N., Md Isa, I., Abu Bakar, S., Saidin, M.I., Ahmad, M.S., Mamat, M., and Hussein, M.Z., 2020, Controlled release formulation of zinc hydroxide nitrate intercalated with sodium dodecylsulphate and bispyribac anions: A novel herbicide nanocomposite for paddy cultivation, *Arabian J. Chem*., 13 (3), 4513–4527.

[19] Jubri, Z., Yusoff, N.Z.A., Marsom, E.S., and Sarijo, S.H., 2009, Controlled release of herbicide into water from Beta-naphtoxyacetic acid-layered double hydroxide nanohybrid formulation, *2009 3rd International Conference on Energy and Environment (ICEE)*, Malacca, Malaysia, 7-8 December 2009.

[20] Sarijo, S.H., Hussein, M.Z, Yahaya, A.H.J., and Zainal, Z., 2010, Effect of incoming and outgoing exchangeable anions on the release kinetics of phenoxyherbicides nanohybrids, *J. Hazard. Mater*., 182 (1-3), 563–569.

[21] Jensen, L.C., Neira-Albornoz, A., and Escudey, M., 2019, "Herbicides Mechanisms Involved in the Sorption Kinetic of Ionisable and Non Ionisable Herbicides: Impact of Physical/Chemical Properties of Soils and Experimental Conditions" in *Kinetic Modeling for Environmental Systems*, Eds. Abdel Rahman, R.O., IntechOpen, Rijeka, Croatia.

[22] Timóteo, T.R.R., de Melo, C.G., Danda, L.J.A., Silva, L.C.P.B.B., Fontes, D.A.F., Silva, P.C.D., Aguilera, C.S.G., Siqueira, L.P., Rolim, L.S., and Rolim Neto, P.J., 2019, Layered double hydroxides of CaAl: A promising drug delivery system for increased dissolution rate and thermal stability of praziquantel, *Appl. Clay Sci*., 180, 105197.

[23] Geilfus, C.M., 2019, Chloride in soil: From nutrient to soil pollutant, *Environ. Exp. Bot.*, 157, 299–309.